FAST COMMUNICATIONS

Contributions intended for this section should be submitted to any of the Co-editors of Acta Crystallographica *or* Journal of Applied Crystallography. *In the letter accompanying the submission authors should state why rapid publication is essential. The paper should not exceed two printed pages (about 2000 words or eight pages of double-spaced typescript including tables and figures) and figures should be clearly lettered. If the paper is available on 5.25" IBM PC compatible or 3.5" Apple /Macintosh diskettes it would be helpful if these could be sent with the manuscript together with details of the word-processing package used. Papers not judged suitable for this section will be considered for publication in the appropriate section of* Acta Crystallographica *or in* Journal of Applied Crystallography.

Acta Cryst. (1993). A**49**, 679-682

First observation of bulk magnetic scattering using high-energy X-rays

BY T. BRÜCKEL,[1]* M. LIPPERT,[2] R. BOUCHARD,[2] T. SCHMIDT,[2] J. R. SCHNEIDER[2] AND W. JAUCH[3]

[1] *Institut für Kristallographie, Charlottenstrasse* 33, *D*-7400 *Tübingen, Germany*

[2] *Hamburger Synchrotronstrahlungslabor HASYLAB at Deutsches Elektronen-Synchrotron DESY, Notkestrasse* 85, *D*-22607 *Hamburg, Germany*

[3] *Hahn-Meitner Institut, Glienickerstrasse* 100, *D*-1000 *Berlin* 39, *Germany*

(*Received* 23 *February* 1993; *accepted* 6 *April* 1993)

Abstract. Today, the most powerful methods for the investigation of magnetic structures are magnetic neutron diffraction and synchrotron-X-ray scattering in the energy range 3-15 keV. This paper reports the first successful experiment to exploit a new technique: the magnetic diffraction of hard X-rays with energies exceeding 80 keV. This technique combines some of the advantages of each of the aforementioned methods: namely high Q-space resolution (10^{-4} Å^{-1} radial and 10^{-5} Å^{-1} tangential) and bulk sensitivity (absorption length >> 1 mm). It is shown that, compared to nominally 10 keV X-ray scattering, enhancement factors of several orders of magnitude can be obtained for the magnetic signal, owing to the increase in penetration depth. The magnetic cross section for these very hard X-rays is discussed, the new technique is compared with the existing methods and a preliminary experiment on MnF_2 is reported.

Introduction. For many years, magnetic neutron diffraction has been a unique tool for the investigation of magnetic structures, magnetic phase transitions and disorder phenomena (Sköld & Price, 1987). While neutron and X-ray diffraction complement each other in structural studies, magnetic X-ray diffraction as discovered by de Bergevin & Brunel (1972, 1981) was, for a long time, considered to be an exotic topic, the magnetic X-ray scattering intensity being reduced by a factor of about 10^{-6} compared with the charge scattering. Only recently has the magnetic X-ray diffraction cross section been exploited for the study of solid-state magnetism, as a result of the availability of very intense and tunable X-ray beams from electron storage rings (Gibbs, 1992). Magnetic synchrotron-radiation diffraction provides a superior Q-space resolution compared with neutron diffraction. However, it suffers from the extremely small nonresonant cross section. This drawback can largely be overcome for actinides and, to a certain extent, for lanthanides by the resonance enhancement at the absorption edges. There remains the problem that, with X-rays in the 1 Å wavelength range, one probes only the near-surface region, while neutrons are diffracted from the bulk material. For certain magnetic-disorder phenomena, a near-surface region can behave quite differently from the bulk material. This has been clearly demonstrated for the random-field Ising magnet $Mn_{0.75}Zn_{0.25}F_2$ (Hill, Thurston, Erwin, Ramstad & Birgeneau, 1991), which, on field cooling, develops a short-range domain state in the bulk but has a second-order transition to true long-range order within a few μm of the surface. In such cases, the phenomenon must be studied on different length scales using complementary techniques.

One possible approach to surmount the shortcomings of conventional X-ray diffraction is the application of high-energy X-rays ($E \gtrsim 80$ keV) for magnetic scattering. In the 0.1 Å wavelength range, absorption becomes very small and diffraction occurs truly from the bulk of the sample. A gain of several orders of magnitude can be achieved for the cross section as a result of the increase in penetration depth. In contrast to the resonance enhancement observed for rare-earth elements, this intensity gain applies for all magnetic materials.

* Present address: HASYLAB at DESY, Notkestrasse 85, D-22607 Hamburg, Germany.

ISSN 0108-7673 © 1993

In this paper, we present the magnetic X-ray cross section for these high-energy X-rays, compare the new method with magnetic neutron and X-ray diffraction and demonstrate the feasibility of this approach through an initial experiment on MnF_2.

The magnetic cross section for high-energy X-rays. Our discussion is based on the expressions for the magnetic X-ray scattering cross section given in equations (12) to (17) in a paper by Blume & Gibbs (1988). These expressions are valid in a nonrelativistic approximation for the electrons and in the limit of high photon energies. With Bragg's law, the cross sections for high-energy photons can be expanded up to the first order in the wavelength, λ, to yield

$$(\mathrm{d}\sigma/\mathrm{d}\Omega)_{\text{magnetic}} = (\lambda_c^2/d^2)\{|S_2|^2 + (\lambda/d)\{P_\eta \times [(L_1'' + S_1'')S_2' - (L_1' + S_1')S_2'']\}\} \quad (1)$$

for pure magnetic scattering and

$$(\mathrm{d}\sigma/\mathrm{d}\Omega)_{\text{interference}} = (\lambda_c/d)\{2(\rho' S_2'' - \rho'' S_2') - P_\eta(\lambda/d)[\rho'(L_1' + S_1') - \rho''(L_1'' + S_1'')]\} \quad (2)$$

for the magnetic and charge interference term.

For simplicity, the cross sections are given in units of the square of the classical electron radius, $(e^2/m_e c^2)^2$. $\lambda_c = h/m_e c = 0.024263$ Å is the Compton length of an electron and d is the lattice spacing of the magnetic reflection under consideration. $S_j = S_j' + iS_j''$ and $L_j = L_j' + iL_j''$ represent the components of the complex Fourier transforms of the spin- and orbital-momentum densities, respectively; $\rho = \rho' + i\rho''$ correspondingly represents the components of the complex Fourier transform of the charge density. As detailed in Blume & Gibbs (1988), the orthonormal coordinate system is chosen such that S_2 and L_2 are the components perpendicular to the scattering plane and S_3 and L_3 are the components antiparallel to the scattering vector, **Q**. The polarization dependence is described by the Poincaré-Stokes vector $\mathbf{P} = (P_\xi, P_\eta, P_\zeta)$.

We first give a short discussion of the interference term before concentrating on the pure magnetic cross section. The leading term of the interference cross section can only be exploited for a noncentrosymmetric magnetic structure with $S_2'' \neq 0$ because, in general, anomalous scattering with $\rho'' \neq 0$ vanishes at these high photon energies. The contribution arising from the circular polarized component ($P_\eta \neq 0$) is appreciably suppressed by a factor of ten or more owing to the λ/d dependence, but can very easily be accessed experimentally. The method involves a flipping of the spins by an applied magnetic field in the scattering plane, a geometry that is particularly easy to realize because of the small scattering angles.

For the pure magnetic scattering cross section, one can estimate that, in the Q range of interest (determined by the form-factor decay), the linear terms amount in general to only 5% of the total cross section. Here, one assumes that the sample orientation is chosen such that $|S_2|$ is maximal. Quadratic and higher-order terms in λ are in most cases negligible. Thus, to a good approximation, one is left with the very simple expression

$$(\mathrm{d}\sigma/\mathrm{d}\Omega)_{\text{magnetic}} = (\lambda_c^2/d^2)|S_2^2|. \quad (3)$$

A comparison of the possibilities of regular and high-energy magnetic X-ray diffraction can be made on the basis of (1), (2) and (3):

(i) *Polarization effects.* In contrast to normal magnetic X-ray diffraction, the leading terms of the cross sections in (1) and (2) show no polarization dependence, as could be expected from the small angles of reflection. $\sigma \rightarrow \pi$ scattering is suppressed in comparison with $\sigma \rightarrow \sigma$ scattering by a factor $\simeq (\lambda/2d)^2$, which amounts to 10^{-3} in typical cases. While this fact simplifies the experimental setup, it hampers the identification of a magnetic signal by means of polarization analysis. However, for a sample having a simple domain structure (*e.g.* MnF_2), magnetic scattering can be identified by rotating the sample around the scattering vector, thus changing the magnitude of the spin component S_2.

(ii) *Separation of* **L** *and* **S.** Because in the approximation of (3) the magnetic cross section depends on the spin moment only, the separation of the magnetic structure factor into spin and orbital components can be achieved quite easily by combining the results of a high-energy X-ray diffraction experiment and a neutron experiment (which is sensitive to **L** + 2**S**) obtained with the identical sample. There is no need for a polarization analysis of the scattered beam.

(iii) *Additional features.* Some features of the regular magnetic scattering cross section are lost: namely resonance enhancement effects, **L** and **S** interference scattering and scattering owing to orbital momentum. However, the simplicity of (3) might make high-energy diffraction a routine tool.

(iv) *Volume enhancement.* Owing to the large penetration depth of high-energy photons, enhancement factors for the cross section of several orders of magnitude (typically 10^3) can be obtained. At present, these gain factors are mostly compensated for by the spectral distribution of the incident photon flux, a disadvantage that will disappear with the installation of spectrometers at storage rings with higher critical energies. For example, with an undulator at the storage ring PETRA (DESY), operating at 14 GeV and 60 mA, one would expect a spectral flux of the order of 10^{15} photons s^{-1} (0.1% bandwidth)$^{-1}$ for 100 keV photons, *i.e.* about five orders of magnitude higher than the flux available in the present experiment. Moreover, for the large and rather perfect crystals required to take advantage of the high

Q-space resolution, this volume enhancement applies fully for weak signals such as those due to magnetic diffuse scattering, while the Bragg charge scattering originates only from a finite volume determined by the extinction length. Therefore, a relative amplification of weak signals can be obtained. As already mentioned in the *Introduction*, for the observation of certain magnetic disorder phenomena, the complementary observation of scattering from the bulk and scattering from a near-surface region is essential.

(v) *General advantages of high-energy diffraction.* These include: the windowless sample environment, as for neutron diffraction; the possibilities of performing magnetic measurements on an absolute scale (absorption and extinction effects become negligible) and of using the same sample for X-ray and neutron studies; and the possibility of detecting weak signals from competing phenomena.

Experimental. To investigate the possibilities offered by the proposed technique, we performed a feasibility study on the new three-crystal diffractometer for hard X-rays on beamline L at HASYLAB (Bouchard, Schneider & Weichert, 1993). The experiment was performed at an X-ray energy of 80 keV using annealed Si 111 crystals, with a rocking-curve width of $\simeq 7.5''$, as monochromator and analyzer crystals (Schneider *et al.*, 1989). As a test sample, we chose the crystal of MnF_2 already studied in earlier experiments on the HASYLAB beamline W1 (Brückel, Lippert, Rilling, Schneider & Prandl, 1993). ω scans performed at the 200 and 020 reflections revealed a sample mosaic width of about $18''$. The plate-shaped crystal was mounted with the c axes vertical in a helium cryostat. For reflections of the type $h00$, the beam path length through the sample was about 15 mm, in contrast to the absorption length of 15 μm at $\lambda = 1.5$ Å. A higher-order component resulting from the 'forbidden' Si 222 reflection could clearly be observed. We used the $\lambda/2$ diffraction from the charge peak 200 as a marker for the position of the magnetic 100 Bragg reflection. For the observation of the magnetic signal, this $\lambda/2$ component could be completely suppressed by setting appropriate electronic windows.

Because multiple scattering can give rise to order-parameter-type temperature dependence, we took special care to avoid this effect. At these high energies, the Ewald sphere is rather large. Moreover, in a double-crystal setup, the sphere broadens rapidly as one moves away from the origin of the reciprocal lattice. Therefore, a continuum of multiple scattering occurs from a whole ensemble of higher-order Bragg peaks. This scattering, however, has a negligible temperature dependence below 100 K, because changes in the lattice parameters [$\Delta a/a < 0.01\%$, $\Delta c/c < 0.1\%$ (Haefner, 1964)] are small compared to the thickness of the Ewald sphere and the Debye-Waller factor is dominated by the zero-point oscillations. Only multiple scattering involving low-indexed reflections can produce a strong temperature change of the intensity. Because at 80 keV the Ewald sphere is essentially planar around $\mathbf{Q} = 0$, the Renninger effect involving reflections with small indices depends very strongly on small tilts of the sample. Therefore, we mounted the whole cryostat on a double-tilt goniometer and studied the 100 intensity when the sample was turned around the scattering vector $\mathbf{Q}$. Within several degrees, no intensity change could be detected.

Results. Fig. 1 shows ω scans of the sample around the 100 position at several temperatures, together with the $\lambda/2$ contribution from 200 as a reference. A very broad

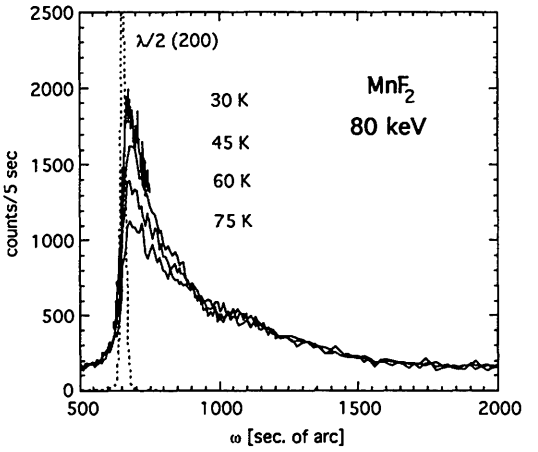

Fig. 1. ω scans around the 100 position at various temperatures, together with the second harmonic signal from 200.

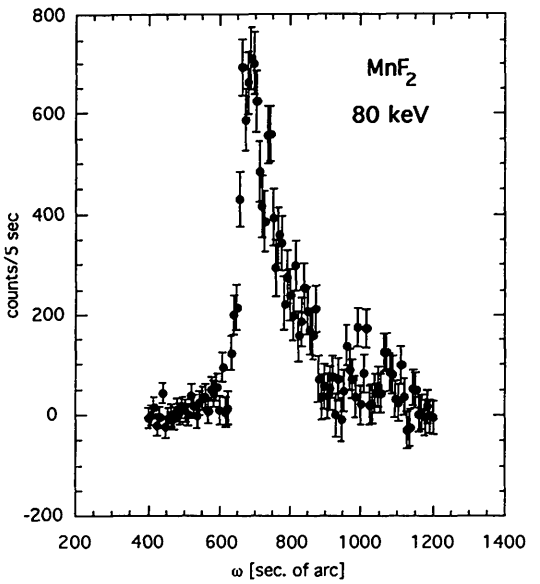

Fig. 2. Difference intensity between 45 and 75 K, which we attribute to magnetic Bragg scattering.

asymmetric feature can be observed. The peak around the 100 position is strongly temperature dependent below T_N = 67.5 K, while above T_N, at temperatures up to 100 K, only small changes can be detected. As detailed above, we believe that, in this temperature interval, an intensity increase of nearly 100% cannot be caused by variations of multiple scattering. The high-angle tail of the intensity distribution does not change in the entire temperature range. It is tempting, therefore, to attribute the temperature variation to a magnetic signal. This signal can be extracted as a difference between low temperatures and $T>T_N$, and is plotted in Fig. 2. For the few temperatures investigated, the integrated intensities of these peaks match well the sublattice magnetization curve reported in the literature for neutrons (Erickson, 1953) and X-rays (Goldman *et al.*, 1987) and measured for the same sample on the W1 beamline (Brückel, Lippert, Rilling, Schneider & Prandl, 1993). This is depicted in Fig. 3 and makes us confident that it is actually magnetic scattering that we are observing. The width of these peaks is roughly 100″, in contrast to the mosaic width of 18″.

Discussion and concluding remarks. In summary, we have proposed a new technique for structural magnetic investigations. We have discussed its potential in comparison with other methods. For the first time, we have observed magnetic diffraction of high-energy X-rays from the bulk of a single crystal. Our result for the width of the magnetic Bragg peak shows that magnetic correlation lengths are smaller than the structural mosaic blocks, a feature that has also been discovered in other materials (Brückel, Prandl & Convert, 1987). The observed width corresponds to antiferromagnetic domain sizes of about 3500 Å, greater than standard neutron diffraction resolutions. In contrast, resolution-limited Bragg peaks were found for near-surface scattering of 6–12 keV photons (Goldman *et al.*, 1987; Brückel, Lippert, Rilling, Schneider & Prandl, 1993). This indicates that large domains of more than 10 000 Å in linear dimension are attached to the surface, which is the crystal's biggest defect.

Owing to time constraints, we could not resolve the nature of the asymmetric background. One possibility is that it is the result of a continuum of multiple Bragg reflections occurring for this particularly large Ewald sphere. One can also speculate that some structural-defect scattering connected with the magnetic phase transition is being observed, in a similar way as has been observed in holmium (Bohr, Gibbs, Moncton & D'Amico, 1986). Obviously, for a neutron diffraction study, such an effect would always remain hidden under the large magnetic signal. Here, high-energy X-ray diffraction might provide additional valuable information. The origin of the broad background scattering will be the subject of further studies.

We conclude that high-energy magnetic X-ray diffraction has a large and, as yet, unexploited potential. We believe that it will become a competitive and complementary tool for the investigation of magnetic long- and short-range order.

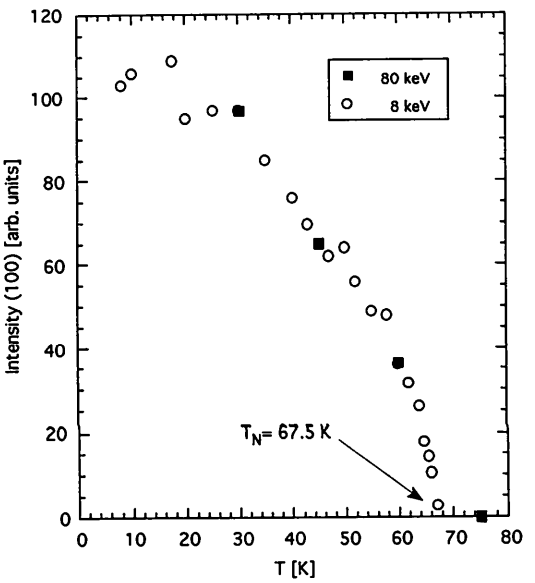

Fig. 3. Temperature dependence of the integrated intensity of the magnetic 100 reflection from MnF_2, as determined from magnetic X-ray diffraction at 8 keV [beamline W1; results represented by open circles (Brückel, Lippert, Rilling, Schneider & Prandl, 1993)] and 80 keV (beamline L; results represented by filled squares). The comparison involves a scale factor determined from the measurement at 45 K.

We have benefited from discussions with W. Prandl. This work was supported by BMFT, grant 03-PR2TUE-3.

References

Bergevin, F. de & Brunel, M. (1972). *Phys. Lett.* **A39**, 141–142.

Bergevin, F. de & Brunel, M. (1981). *Acta Cryst.* **A37**, 314–324.

Blume, M. & Gibbs, D. (1988). *Phys. Rev. B*, **37**, 1779–1789.

Bohr, J., Gibbs, D., Moncton, D. E. & D'Amico, K. L. (1986). *Physica (Utrecht)*, **A140**, 349–358.

Bouchard, R., Schneider, J. R. & Weichert, G. (1993). In preparation.

Brückel, T., Lippert, M., Rilling, V., Schneider, J. R. & Prandl, W. (1993). In preparation.

Brückel, T., Prandl, W. & Convert, P. (1987). *J. Phys. C*, **20**, 2565–2583.

Erickson, R. A. (1953). *Phys. Rev.* **90**, 779–785.

Gibbs, D. (1992). *Synchrotron Radiat. News*, **5**, 18–23.

Goldman, A. I., Mohanty, K., Shirane, G., Horn, P. M., Greene, R. L., Peters, C. J., Thurston, T. R. & Birgeneau, R. J. (1987). *Phys. Rev. B*, **36**, 5609–5612.

Haefner, K. (1964). PhD thesis, Univ. of Chicago, Illinois, USA.

Hill, J. P., Thurston, T. R., Erwin, R. W., Ramstad, M. J. & Birgeneau, R. J. (1991). *Phys. Rev. Lett.* **66**, 3281–3284.

Schneider, J. R., Nagasawa, H., Berman, L. E., Hastings, J. B., Siddons, D. P. & Zulehner, W. (1989). *Nucl. Instrum. Methods*, **A276**, 636–642.

Sköld, K. & Price, D. L. (1987). Editors. *Neutron Scattering*. New York: Academic.